Polym. Bull. (2012) 68:2071–2087
DOI 10.1007/s00289-012-0723-0

ORIGINAL PAPER

Triple percolation behavior and positive temperature coefficient effect of conductive polymer composites with especial interface morphology

Chang Lu · Xiao-ning Hu · Yu-xin He · Xinhui Huang · Ji-chun Liu · Yu-qing Zhang

Received: 19 December 2011 / Revised: 8 February 2012 / Accepted: 20 February 2012 /
Published online: 28 February 2012

Abstract Selective localization of carbon black (CB) at the interface of polymer blends was achieved by the method that poly(styrene-*co*-maleic anhydride) (SMA) was first reacted with CB, and then blended with nylon6/polystyrene (PA6/PS). In the PA6/PS blends, CB was localized in PA6 phase and typical double percolation was exhibited. In the PA6/PS/(SMA–CB) blends, TEM results showed that CB particles were induced by SMA to localize at the interface, resulting in the especial interface morphology fabricated by SMA and CB. The especial interface morphology of PA6/PS/(SMA–CB) caused distinct triple percolation behavior and very low percolation threshold. The positive temperature coefficient (PTC) intensity of PA6/PS/(SMA–CB) composites was stronger than that of PA6/PS/CB and the negative temperature coefficient (NTC) effect was eliminated. The elimination of NTC effect was arisen from the especial interface morphology. A stronger PTC intensity was attributed to the low percolation threshold and the morphology.

Keywords Polymer blends · Carbon black · Morphology · Electrical conductivity · PTC effect

Introduction

It is well known that conductive polymer composites (CPCs) can be produced by adding a critical amount of carbon black (CB), which is referred to as the percolation threshold, in an insulating polymer. CPCs have many applications, including antistatic materials, positive temperature coefficient (PTC) materials characterized by a reversible conductor to insulator transition at a defined

C. Lu (✉) · X. Hu · Y. He · X. Huang · J. Liu · Y. Zhang
Key Lab of Polymer Science and Nanotechnology, Chemical Engineering & Pharmaceutics School, Henan University of Science and Technology, Luoyang 471003, China
e-mail: luchang139@126.com

temperature, electromagnetic shielding, and chemical vapor detection [1, 2]. However, there are some application limits because of the several drawbacks of CPCs produced by CB filled an insulating polymer. They are (1) the high percolation threshold which affects the composite mechanical properties, processability and increases the cost of the final composite, (2) strong negative temperature coefficient (NTC) effect which exhibits a large decrease in resistance around a defined temperature.

In recent years, CB-filled immiscible polymers have received increasing attention because it is the most promising method to reduce the percolation threshold. The decrease of percolation threshold can be attributed to the double percolation resulting from the selectively distribution of CB in one of the two phases or at the interface of the polymers [3–9]. Obviously, the localization of CB at the interface of the two phases can provide a composite with the lowest percolation threshold.

It has been known that as long as the viscosities of two polymers are comparable, affinity of CB for each component is the main factor determining uneven distribution of CB in polymer blends. Although the selective localization of the CB at the interface can provide a composite with the lowest percolation threshold, very few investigations about controlling CB localization at the interface were reported due to the affinity of CB for polymer matrix more than for interface. Even so a few methods to prepare CPCs of CB localization at the interface were reported. Gubbels [10] employed a kinetic strategy to localize CB at the interface of PS/PE blends. As per the results, the percolation threshold of composites is only 0.4 wt%, being one of the lowest percolation threshold reported in the open literature. And Li and coworkers [11] also employed this method to prepare the PET/PE/CB conductive composites with CB localized at the interface. Feng et al. [12] found that when the viscosities of PP and PMMA were comparable, the CB particles were localized at the interface. Al-Saleh and Sundararaj [13] introduced SBS which localized at the interface of immiscible PS/PP blends and had the highest affinity for CB to induce CB localization at the interface.

Although there is no satisfactory theory to explain the NTC phenomenon, it is widely accepted that the NTC effect is presumably due to the reaggregation of the conductive particles in the polymer melting and the reparation of disconnected conductive pathways [14]. So in the industry the methods that use a crosslinking agent or Gamma and electron beam radiations to crosslink CB-filled polymer composites were applied to prevent the reaggregation of the conductive particles, and to eliminate the NTC effect [15–17]. However, the cross-linking treatment not only increases the processing cost, but also can not resolve the drawback of high percolation threshold. Some researchers [14, 18–20] found that using a very high viscosity polymer as one of the components of CPCs is a good approach to decrease the percolation threshold and remove NTC effect, but the introduction of very high viscosity polymer deteriorates the processability of CPCs.

The objectives of this article include: (1) to obtain a conductive composite with a very low percolation threshold, (2) to provide a new approach to eliminate the NTC effect. To achieve these objectives, an innovational method that poly(styrene-*co*-maleic anhydride) (SMA), the compatibilizer of PS and PA6, was first reacted with CB and then blended with PS/PA6 was employed to prepare CPCs.

Experimental

Materials

The materials used in this study were polystyrene (model PG-383M, MI = 8.5 g/10 min, $d = 1.05$ g/cm^3) supplied by Zhenjiang Chi Mei Chemicals Co., Ltd. and polyamide-6 (PA-6) (model 33500, relative viscosity is 3.50, $d = 1.14$ g/cm^3), supplied by Xinhui Meida-DSM Nylon Chips Co., Ltd. The compatibilizer employed in this study was SMA (MPC1501, Shanghai SUNNY New Technology Development Co., Ltd.). The amount of maleic anhydride in SMA was 18 wt%. A China-made acetylene CB with an average diameter of 45 nm, dibutyl phthalate absorption (DBP) value of 440 mL/100 g, electrical resistivity of 1.8 Ω m, was used as conductive filler.

Preparation of CPCs

Based on the condition of the reaction between hydroxyl group at CB surface and maleic anhydride in the SMA [21], the SMA/CB composites were prepared as follows: SMA and CB with desired proportions were dissolved in dimethylbenzene and then reacted at 120 °C for 24 h. The reactant was deposited with acetone at room temperature and then dried in a vacuum oven at 90 °C for 24 h to remove the solvent. The content of CB in SMA–CB was 20, 30, and 40 wt%.

The CPCs were prepared using a Haake Rheomix series 600 batch mixer at 240 °C and 60 rpm for 10 min. The materials obtained were further compressed into 40 × 40 × 1 mm sheets by a hot press at 230 °C for electricity tests. To reduce contact resistivity, the two sides of the samples were bonded with aluminum foil.

Measurements and characterization

To investigate the amount of SMA reacted with CB, SMA in SMA–CB (80/20) was extracted for 48 h by acetone using Soxhlet extractor. The ratio of SMA reacted with CB was calculated according to Eq. 1.

$$\text{Ratio}\% = \left[1 - \frac{(\text{SMA}-\text{CB})_\text{i} - (\text{SMA}-\text{CB})_\text{f}}{(\text{SMA}-\text{CB})_\text{i} \times 0.8}\right] \times 100\%, \quad (1)$$

where $(\text{SMA–CB})_\text{i}$ and $(\text{SMA–CB})_\text{f}$ are the initial and final mass of SMA–CB, respectively.

The electrical resistivity of conductive composites was measured by using a multimeter when the resistivity was lower than 2×10^7 Ω. The measurements were done by using ZC-36 High Resistance Electrometer when the resistivity exceeded 2×10^7 Ω. The temperature dependence of composites resistivity was measured by heating the samples at a rate of 1 K/min in an oven.

High resolution transmission electron microscopy (HRTEM) was used to examine the size of CB and CB modified with SMA by a JEM 2100F microscope at an acceleration voltage of 300 kV. In the HRTEM measurements of CB and CB

modified with SMA, a drop of the CB dispersions was placed on a Cu grid having size about 3.05 mm in diameter (200 mesh), then vacuum dried to remove trace of water and analyzed. CB modified with SMA was extracted for 48 h by acetone using Soxhlet extractor before using HRTEM to measure.

Transmission electron microscopy (TEM) method was used to examine the localization of CB in PA6/PS/(SMA–CB) by an FEI TECNAI-G20 microscope at an acceleration voltage of 300 kV. Ultra thin sections of 70 nm in thickness were cryogenically cut with a diamond knife at −100 °C to the sample of PS/PA6/(SMA–CB).

The fractured morphology of the composites was examined using JEOL 6301F scanning electron microscope (SEM). The molded specimens were fractured in liquid nitrogen and coated with gold. To get better contrast, the samples were etched by formic acid or dimethylbenzene before coating.

Results and discussion

Percolation behavior of PA6/PS/CB composites

The OM was employed to investigate the distribution of CB in PA6/PS blends, as shown in Fig. 1. The results show that 6 wt% CB-filled PA6/PS (60/40) exhibits co-continuous morphology and CB is selectivity localized in one phase. To investigate the localization of CB, the dimethylbenzene or formic acid was used to extract the PS phase (Fig. 2a) or PA6 phase (Fig. 2b) of PA6/PS/CB composites. It can be seen that the solution of the sample extracted by dimethylbenzene is transparent, while the solution of the sample extracted by formic acid is dark. The results show that CB is localized in PA6 phase, indicating that the affinity of CB for PA6 is stronger than for PS. To confirm this conclusion, the sample etched by dimethylbenzene was investigated by SEM, as shown in Fig. 3. The CB particles can be easily found in the PA6 phase, indicating that CB is selectivity localized in PA6 phase.

The effect of the PA6 concentration on the room-temperature resistivity of 8 wt% CB-filled PA6/PS blends is shown in Fig. 4. The results demonstrate that PA6

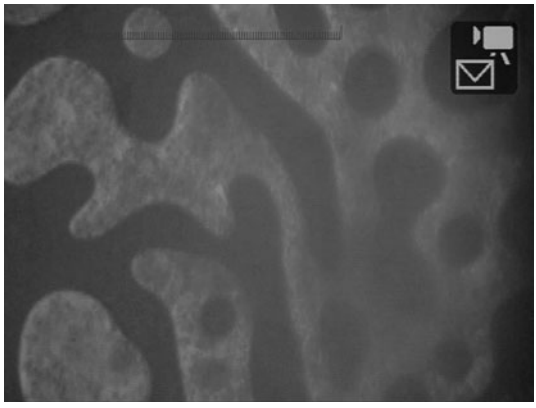

Fig. 1 OM image of 6 wt% CB-filled PA6/PS (60/40) blend

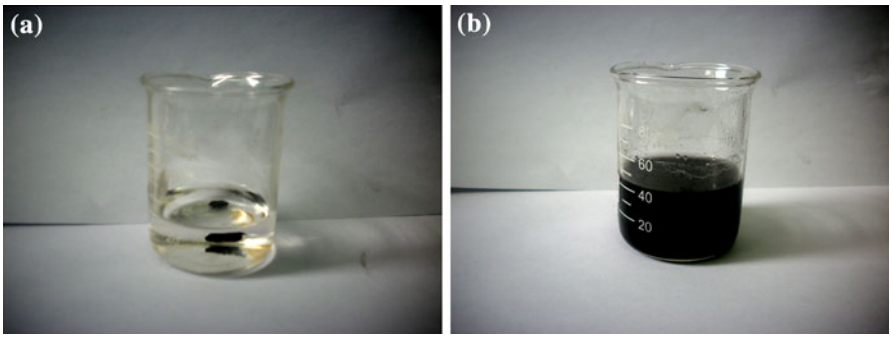

Fig. 2 Solutions obtained by etching 6 wt% CB-filled PA6/PS (60/40) blends with different solvents: **a** dimethylbenzene and **b** formic acid

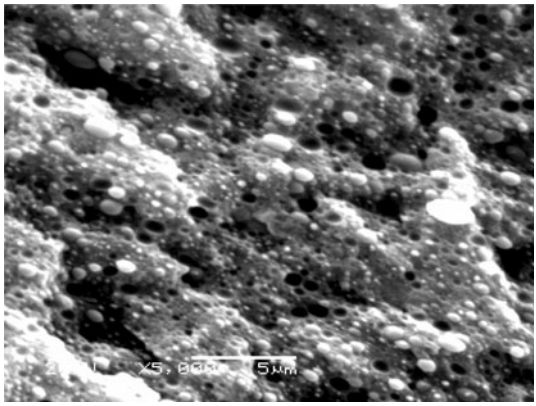

Fig. 3 SEM image of 6 wt% CB-filled PA6/PS (60/40) blend

concentration has a significant effect on the volume resistivity of PA6/PS/CB blends. The blends are insulating when the concentration of PA6 in PA6/PS blends is <20%. And the conductive composites can be prepared as the content of PA6 is at the range of 20–100%, indicating that PA6 phase can form the continuous phase at this range.

Figure 5 shows the influence of CB content on the room-temperature resistivity of PA6/PS/CB composites. At low CB loadings (2–5 wt%), a little change in volume resistivity can be observed because the distances between CB particles are large enough. The volume resistivity falls down sharply from 10^{15} to 10^{7} Ω cm as the CB content increase to 6 wt%, indicating that the percolation threshold of PA6/PS/CB composites is 6 wt%. This indicates that CB particles came into contact with each other or closed up enough to allow the electron hop by tunneling, thus forming continuous conducting path.

From Figs. 4, 5, it can be observed that PA6/PS/CB composites exhibit typical characteristics of double percolation transition. One is concentration of CB in the PA6 phase and the other is PA6 phase continuity.

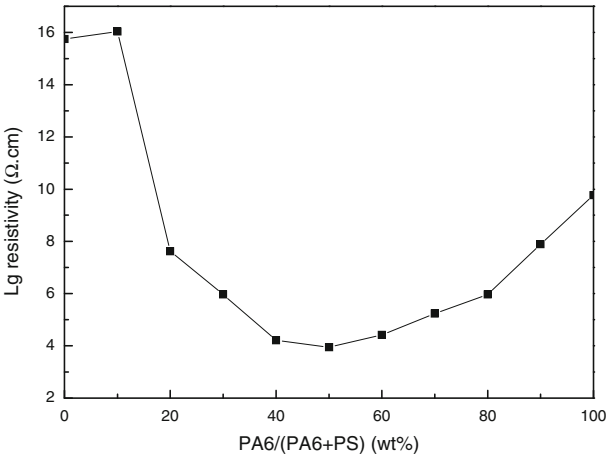

Fig. 4 Effect of the PA6 concentration on the room-temperature resistivity of 8% CB-filled PA6/PS blends

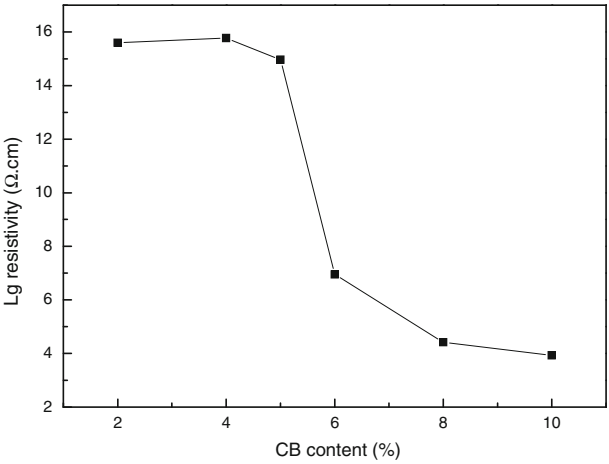

Fig. 5 Effect of CB content on the room-temperature resistivity of CB-filled PA6/PS (60/40) composites

Dispersion of CB in PA6/PS/(SMA–CB) composites

Figure 6 shows typical HRTEM micrographs of CB and CB modified with SMA. The investigation with HRTEM presents that the diameter of CB was larger after modification with SMA, with the diameters increasing from average 40 to 70 nm. These results demonstrate that the CB particles are covered by SMA. Before using HRTEM to measure, CB modified with SMA was extracted for 48 h by acetone to remove SMA which was not reacted with CB. So the increase of diameters indicates that SMA reacted with CB.

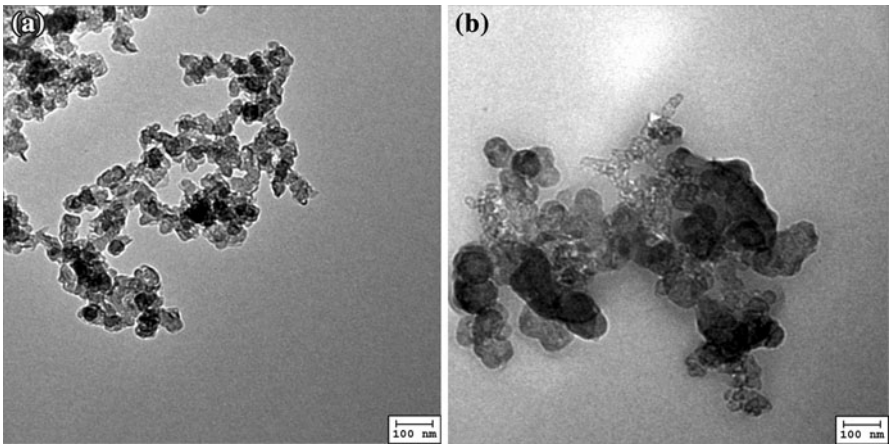

Fig. 6 TEM of CB (**a**) and CB modified with SMA (**b**)

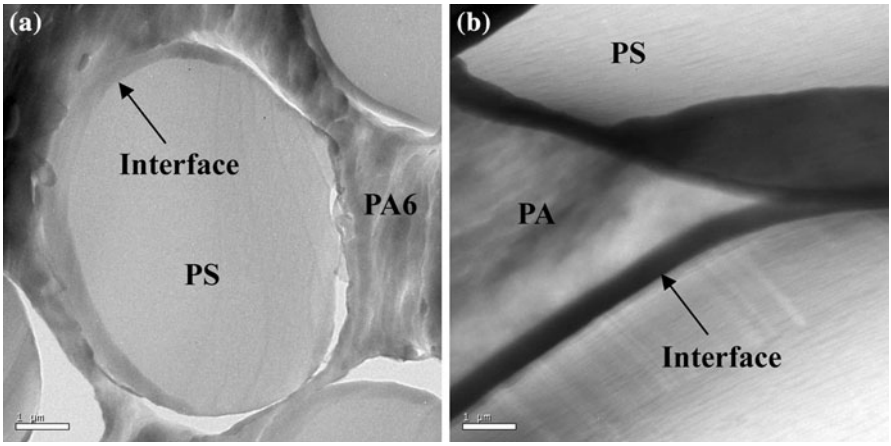

Fig. 7 TEM photograph of PA6/PS/SMA (70/30/2) (**a**) and 2 wt% SMA–CB (70/30) (**b**)-filled PA6/PS (70/30) blends

The results of extracting experiment identify that the remainder of SMA–CB extracted by acetone contains 42% SMA. The residue of SMA in the extracted SMA–CB also indicates that SMA reacted with CB and could not be extracted by acetone.

TEM was applied to investigate the distribution of CB in the composites of PA6/PS/(SMA–CB). From Fig. 7b, it can be observed that PS is the minor phase and is lighter than the PA6 major phase. For 2 wt% SMA–CB (70/30)-filled PA6/PS (70/30) blends, the CB particles are not observed in PS and PA6 phase, indicating that CB did not disperse in matrix. Although the CB particles can not be observed directly at the interface in PA6/PS/(SMA–CB), its color appears darker than in

PA6/PS/SMA(70/30/2), indicating that the CB particles are selectively localized at the interface, resulting in the electron dense.

The localization of CB at the interface of PA6/PS can be attributed to the induced effect of SMA on CB. SMA copolymer, as the compatibilizer of PS/PA6 blends, should congregate at the interface of PA6/PS blends due to the fact that the compatibilizer will selectively localize at the interface of immiscible polymer blends to reduce the interfacial tension. Furthermore, SMA had reacted with CB before being introduced into the PA6/PS blends, so the affinity of CB for SMA stronger than for PA6 and PS. Therefore, the CB particles can be localized at the interface by SMA spontaneously during the processing of PA6/PS/(SMA–CB) blends.

Percolation behavior PA6/PS/(SMA–CB) composites

The localization of CB at the interface induced by SMA indicates that the interface of PA6/PS/(SMA–CB) contains SMA and CB, thus resulting in interface morphology more complicated than that of CPCs of which the interface contains CB only [10–12]. The complicated interface morphology of PA6/PS/(SMA–CB) blends may imply especial electrical properties. Based on this, the percolation behaviors, percolation threshold of PA6/PS/(SMA–CB) composites were investigated.

The effect of PA6 concentration on the room-temperature resistivity of 6 wt% SMA–CB (70/30) composites filled PA6/PS blends is shown in Fig. 8. The electrical conductivity is determined by PA6 concentration. The blends are insulating when the concentration of PA6 in PA6/PS blends is >70 or <10%. The conductive composites can be prepared when the PA6 concentrations are between 10 and 70%.

The morphologies of PA6/PS/(SMA–CB) are investigated by SEM to explain the drastic change of composite conductivity, as shown in Fig. 9. To enhance the

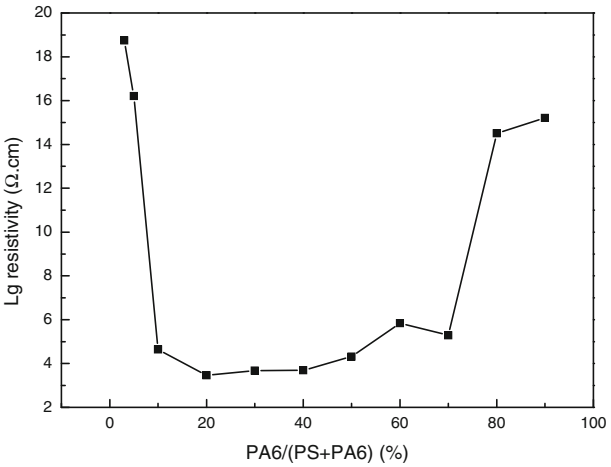

Fig. 8 Effect of the PA6 concentration on the room-temperature resistivity of 6% SMA-CB-filled PA6/PS

contrast, the samples with the PA6 content <40 wt% were etched by formic acid to remove PA6 phase and dimethylbenzene was used to etch PS phase for the PA6 content in the samples >50 wt%. Figure 9a–c shows that the blends with PA6 content <40 wt% have the sea-island morphology in which spherical PA6 particles disperse in continuous PS phase. Figure 9d exhibits the co-continuous morphology of PA6 and PS in the PA6 content of 40 wt%. When the content of PA6 is

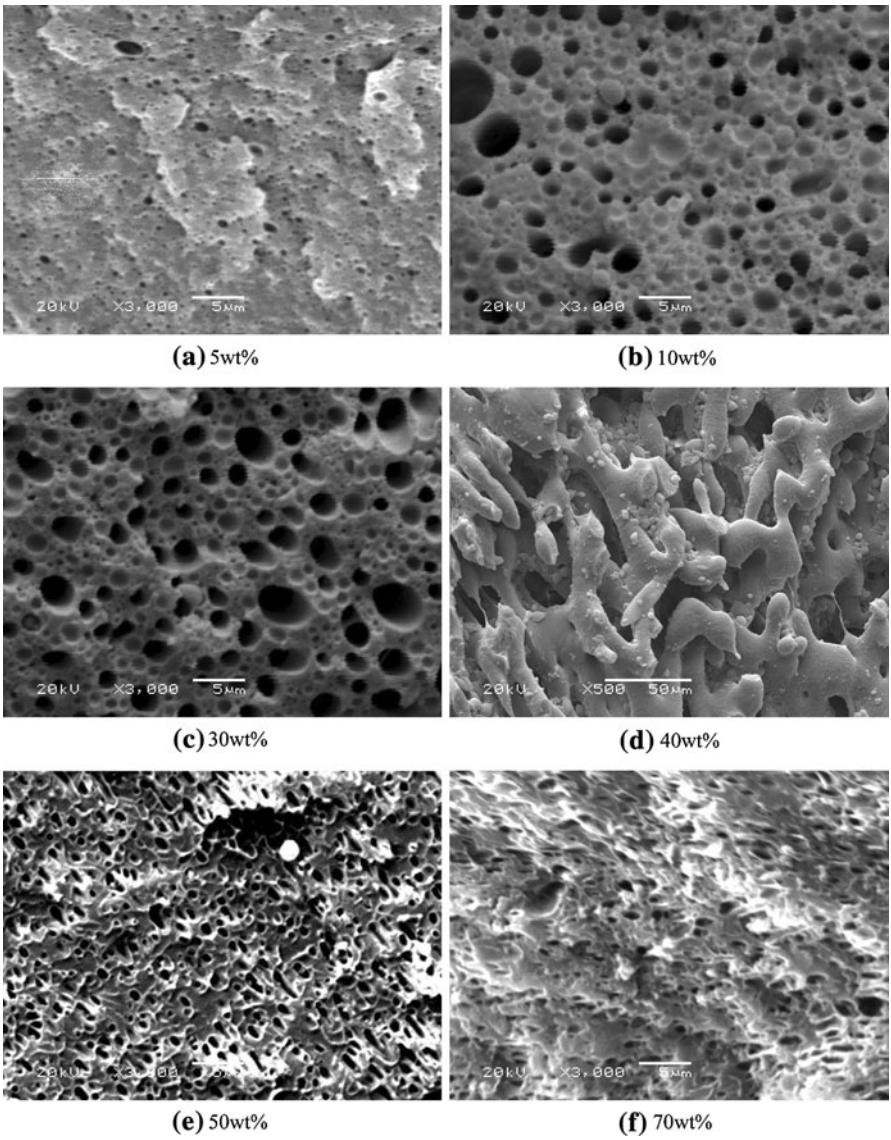

Fig. 9 SEM of 6 wt% SMA-CB-filled PA6/PS at various PA6 contents

>40 wt%, micrographs show a sea-island morphology in which PS is the spherical dispersed phase, as shown in Fig. 9e, f.

Based on Figs. 8 and 9, it can be concluded that the conductive composites of SMA–CB-filled PA6/PS were prepared even when two phases formed sea-island structure in which the shape of dispersed phase is spherical. But according to the literature reported [10–13], for the conductive composites of CB localization at the interface, two phases should form co-continuous morphology [10, 12], or dispersed phase formed microfibrillar or rod-like structure in continuous phase [11, 13].

To explain this phenomenon, the schematic diagrams about the evolvement of conductive network of PA6/PS/(SMA–CB) as the increase of PA6 concentration are shown in Fig. 10. At low PA6 content (<10 wt%), the amount of dispersed PA particles is so scarce that dispersed PA particles are too far apart to fabricate a continuous conductive network (Fig. 10a). As the PA6 concentration is between 10 and 30%, conductive surfaces of dispersed PA6 particles come into contact with each other or closes up enough to allow the electron hop by tunneling, thus forming continuous conducting path (Fig. 10b). PA6/PS co-continuity formed at the PA6 content of 40 wt% indicates that the PA6/PS interface is continuous and the continuous conductive network at the interface can be established by CB, as shown in Fig. 10c. At 50–70 wt% PA6 concentration in PA6/PS, although co-continuous morphology is broken, the conductive surfaces of dispersed PS particles still come into contact with each other to fabricate the continuous conductive network (Fig. 10d). When the PA6 concentration is >70%, the PS concentration is so low

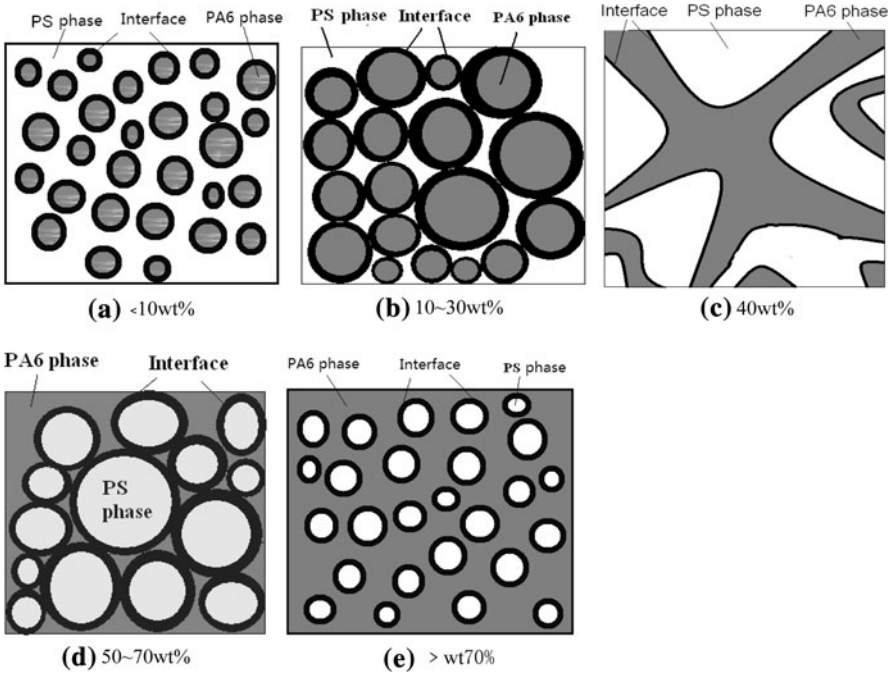

Fig. 10 Schematic morphology of PA6/PS/(SMA–CB) at different PA6 contents

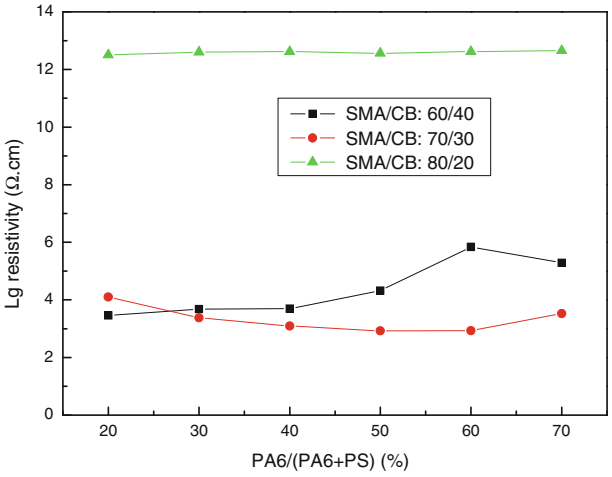

Fig. 11 Influence of SMA–CB ratio on the room-temperature resistivity of PA6/PS blends containing 6 wt% SMA–CB

that the conductive surfaces of dispersed PS particles are separated by continuous PA6 phase, resulting in the breakage of continuous conductive network (Fig. 10e).

Based on the previous discussion, it can be concluded that the percolation caused by the PA6 concentration can be governed by the interface continuity between PS and PA6 phases.

The influence of SMA–CB ratio on the room-temperature resistivity of PA6/PS/(SMA–CB) is studied, as shown in Fig. 11. At 6 wt% SMA–CB loading, electrical resistivity results show that the electrical conductivity of PA6/PS/(SMA–CB) composites is determined by the ratio of SMA/CB. The composites are not conductive at the SMA/CB ratio of 80/20, and the conductive composites can be obtained as the SMA/CB ratios are 70/30 and 60/40. So the percolation phenomena are observed at the ratios of SMA/CB between 80/20 and 70/30. Those percolation phenomena should be attributed to the different aggregation state of SMA molecular chain grafted on CB surface before or after being introduced into the PA6/PS blends. The introduction of SMA–CB composites to the PA6/PS blends should induce the SMA molecular chain from the curled state to uncurled state as a result from the compatibilization of SMA. The extension of SMA molecules at the interface should broaden the distance between CB particles due to the fact that SMA chains are grafted on the CB surface. So for the low ratio of SMA/CB the extension of SMA molecules will lead to the separation of CB particles, resulting in interruption of conductive network. On the contrary, for the high ratio of SMA/CB, the content of CB particles in SMA/CB composites is so high that the CB particles can still contact each other to form the conductive pathway even the SMA chains extend at the interface. Therefore, the percolation phenomenon described above can be attributed to the percolation of CB in SMA–CB.

Influence of SMA–CB (70/30) loading on the room-temperature resistivity of PA6/PS blends with different PA6/PS ratios is reported in Fig. 12. Three PA6/PS

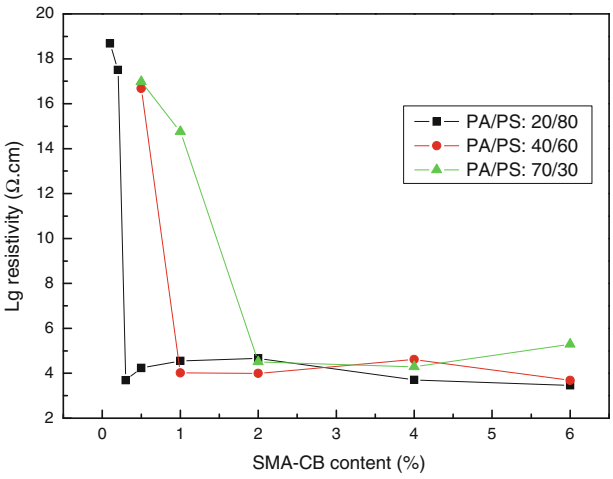

Fig. 12 Effect of SMA–CB (70/30) loading on the room-temperature resistivity of PA6/PS/(SMA–CB) composites

ratios are studied: 20/80, 40/60, and 70/70. For all blends studied, similar electrical resistivity curves for different PA6/PS blend ratios are observed: a dramatic decrease in resistivity near the critical SMA–CB loading, indicating that the percolation of PA6/PS/(SMA–CB) composites is governed by the concentration of SMA–CB. The percolation phenomenon should be attributed to the continuity of SMA–CB at the interface. At the SMA–CB loading lower than critical SMA–CB loading, the distribution of SMA–CB at the interface is noncontinuous due to the very low loading, resulting in the discontinuity of conductive network. As the loading of SMA–CB is increased to the critical SMA–CB loading, SMA–CB can fill the interface to form a continuous conductive network.

From the above investigation, it can be concluded that the percolation of PA6/PS/(SMA–CB) composites is governed by the three factors, i.e., the continuity of SMA/CB at the interface, the percolation of CB in SMA phase, and the interface continuity of PS and PA6, which can be defined as triple percolation, a notable difference from double percolation and seldom reported in literature.

In Fig. 12, it is observed that a dramatic decrease in resistivity is at a critical SMA–CB loading of 0.3 wt% (PA6/PS: 20/80), 1 wt% (PA6/PS: 40/60), and 2 wt% (PA6/PS: 70/30). Considering that the mass ratio of SMA/CB is 70:30, it is can be calculated that the percolation thresholds of PA6/PS/(SMA–CB) composites are 0.09 wt% (PA6/PS: 20/80), 0.3 wt% (PA6/PS: 40/60), and 0.6 wt% (PA6/PS: 70/30). These percolation thresholds of PA6/PS/(SMA–CB) are much lower than that of PA6/PS/CB composites. It should be pointed out specially that the percolation threshold of the composites (PA6/PS: 20/80) is only 0.09 wt% of CB, which is the lowest percolation threshold reported in the open literature. The localization of CB and SMA at the interface is the main reason for the very low percolation threshold, as well as the percolation of CB in SMA–CB and the percolation of SMA–CB at the interface are also beneficial to the decrease of

percolation threshold, namely the very low percolation threshold can be owed to the triple percolation arising from the special interface morphology.

PTC effect of PA6/PS/(SMA–CB) composites

The especial morphology of PA6/PS/(SMA–CB) blends may imply especial PTC effect. Based on this, PTC effect of PA6/PS/(SMA–CB) composites was investigated subsequently. In fact, the desired CPCs serving as PTC materials should have a filler concentration a bit higher than the upper limit of the percolation region. Accordingly, the samples of 6 wt% CB-filled PA6/PS (60/40), 0.3 wt% SMA–CB (70/30)-filled PA6/PS (20/80), 1 wt% SMA–CB (70/30)-filled PA6/PS (40/60), and 2 wt% SMA–CB (70/30)-filled PA6/PS (70/30) were chosen to test their temperature dependence of the resistivity.

From Fig. 13, it is observed that the resistivity of PA6/PS/CB blend shows a weak jump at about 170 °C followed by the NTC effect at 185 °C. It was identified the localization of CB in PA phase. So the PTC effect of PA6/PS/CB blend can be attributed to a significant volume expansion of PA phase near its melting temperature (T_m), leading to the disconnection of CB in PA6. The appearance of NTC effect can be arisen from the CB reagglomeration to form the conductive pathways again.

From Fig. 13, it can be observed that the temperature dependence of the resistivity of PA6/PS/(SMA–CB) is different from that of PA6/PS/CB. The PTC effect of PA6/PS/(SMA–CB) composites occurs near PA6 T_m and the intensity is higher than that of PA6/PS/CB. Moreover, the volume resistivity shows a slow increase or decrease as the temperature increase, indicating that the NTC effect is eliminated.

According to the PTC mechanism [22–24], the PTC effect of CB-filled polymer produced by the conventional melt-mixing method is caused by the melting of the matrix. The melting of the matrix makes a significant volume expansion, which increases the interparticle gaps of the conductive particles and reduces the number

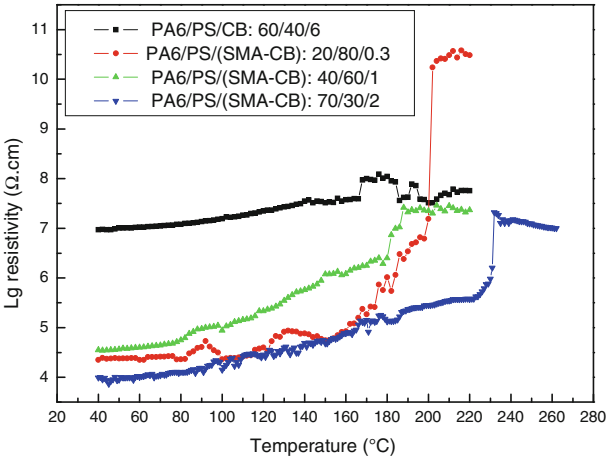

Fig. 13 Temperature–resistivity curves of PA6/PS/CB and PA6/PS/(SMA–CB)

of conductive pathways, resulting in a dramatic increase in the resistivity. For the PA6/PS/(SMA–CB) composites the conductive pathways is confined at the interface and narrower than of PA6/PS/CB, which can be broken up by a slight volume expansion, resulting in a strong PTC effect.

The NTC effect is believed to be due to the reaggregation of conductive particles in the polymer melt and the reparation of the disconnected conductive pathways. The relatively free movement of conductive particles occurs only when the viscosity of the polymer is sufficiently low. The elimination of NTC effect in PA6/PS/(SMA–CB) composites can be explained by its especial interface morphology: CB particles and SMA molecular chains dispersed at the interface, the SMA molecular chains were grafted on the surface of CB particles and the maleic anhydride in the SMA was reacted with amine group of PA6 to form the copolymer. When the temperature is lower than the T_m of PA6, the CB particles are fixed by freezing PA molecular chains, prohibiting the reagglomeration of CB particles at the interface. When the temperature is higher than the T_m of PA6, although the viscosity of the matrix decrease greatly, the reagglomeration of CB particles is still hard to occur due to the fact that the PA and SMA molecular chains were grafted on the surface of CB particles and enlarged the motion resistance of CB particles, leading to the elimination of NTC effect.

Compared with the temperature dependence of the resistivity of PA6/PS/(SMA–CB) composites each other, it can be observed that PA6/PS/(SMA–CB) (20/80/0.3) has the strongest the PTC intensity and the weakest PTC intensity was observed in PA6/PS/(SMA–CB) (70/30/2). A high PTC intensity may suggest a weaker conductive network in the composites, which can be broken up by a slight volume expansion. So generally, low CB content composites show a higher PTC intensity. The high PTC intensity of PA6/PS/(SMA–CB) (20/80/0.3) can be attributed to the lowest percolation threshold. But the PTC intensity of 40/60/1 is lower than that of 70/30/2, even its percolation threshold lower than that of 70/30/2. So there might be other factors to influence the PTC intensity.

From Fig. 9, it has been known that the morphology of PA6/PS/(SMA–CB) (40/60/6) is different from the morphology of 70/30/6. This implied that the difference of morphology might be the factor to influence the PTC intensity. Based on this, SEM was employed to investigate the morphology of PA6/PS/(SMA–CB) composites at a critical SMA–CB loading, as shown in Fig. 14. The sample with the PA6/PS ratio of 20/80 was etched by formic acid to remove PA6 phase and the samples with the PA6/PS ratio of 40/60 and 70/30 were etched by dimethylbenzene to remove PS phase. From Fig. 14, it is observed that the morphologies of PA6/PS blends at a critical SMA–CB loading are similar to the PA6/PS blends at 6 wt% SMA–CB loading. Blend with PA6/PS ratio of 20/80 has the morphology of PA6 dispersed in PS (Fig. 14a). The PA6/PS co-continuity was observed in the PA6 content of 40% (Fig. 14b). When the content of PA6 is 70%, micrographs show a two-phase morphology in which PS is the dispersed phase (Fig. 14c).

In the composites of PA6/PS/(SMA–CB) (20/80/0.3) and (70/30/2) with sea-island morphology, the conductive network was formed by the method that the conductive surfaces of dispersed phase contact each other. Compared with the conductive network formed by co-continuous morphology, the conductive network formed by sea-island morphology is easier to be broken up due to the fact that the

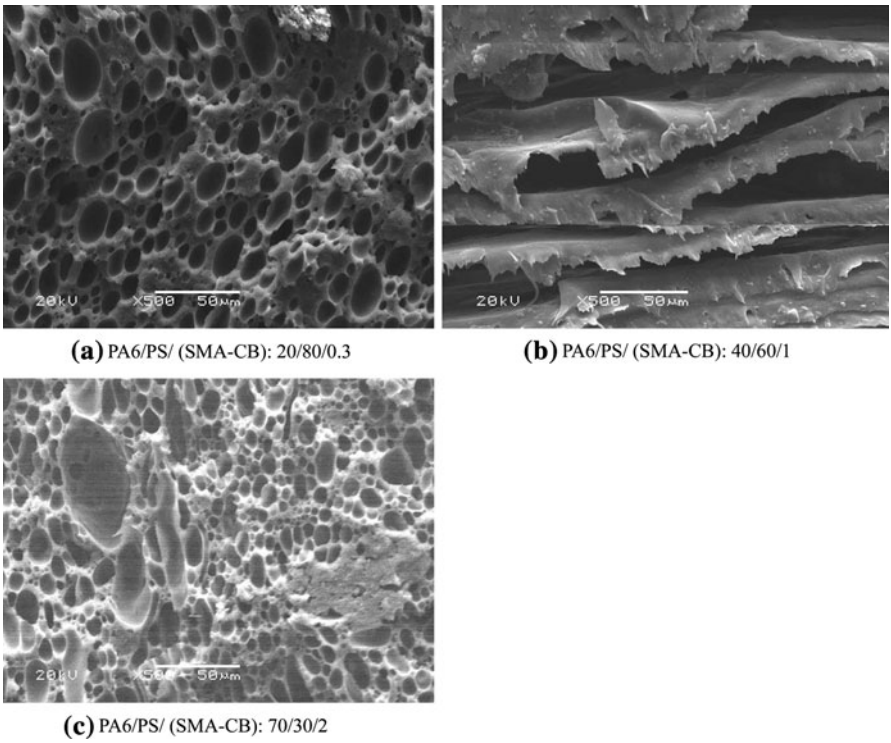

Fig. 14 SEM of PA6/PS/(SMA–CB) composites in different PA6/PS ratio at a critical SMA–CB loading

entire conductive network should be destructed as long as the conductive point formed by the contact of dispersed phase was interrupted. A weaker conductive network can cause a higher PTC intensity. So the strongest PTC intensity of PA6/PS/(SMA–CB) (20/80/0.3) can be attributed to the lowest percolation threshold and sea-island morphology. Although the percolation threshold of PA6/PS/(SMA–CB) (70/30/2) is higher than that of PA6/PS/(SMA–CB) (40/60/1), its sea-island morphology causes that the conductive network is easier to break up by a slight volume expansion, resulting in a higher PTC intensity.

The PTC effect of PA6/PS/(SMA–CB) composites is caused by the volume expansion of the PA6 phase near its T_m. Obviously, a high PA6 content in PA6/PS/(SMA–CB) can cause a large volume expansion, resulting in a higher PTC intensity. So besides the effect of morphology on the PTC intensity, the higher PA6 content is another factor to cause the PTC intensity of PA6/PS/(SMA–CB) (70/30/2) higher than that of PA6/PS/(SMA–CB) (40/60/1).

Conclusions

An innovational method that SMA, a compatibilizer of PA6/PS blends, was first reacted with CB and then blended with PA6/PS, has been employed to prepare the

PA6/PS/(SMA–CB) composites of which CB localized at the interface. In PA6/PS/CB blends, CB was found to preferentially localize in the PA6 phase. The composites exhibited typical characteristics of double percolation. However, for the PA6/PS/(SMA–CB) composites, CB was induced by SMA to localize at the interface of PA6/PS, resulting that the interface was fabricated by SMA and CB. The especial interface morphology of PA6/PS/(SMA–CB) caused interesting conductive structure and electrical properties. Continuous conductive network was formed not only in the morphology with co-continuous structure, but also in the morphology with sea-island structure. The PA6/PS/(SMA–CB) composites exhibited distinct triple percolation behavior, i.e., the percolation is governed by the percolation of CB in SMA phase, the continuity of SMA–CB at the interface and the continuity of PA6/PS interface. The percolation threshold of PA6/PS/(SMA–CB) was much lower than that of PA6/PS/CB. The PTC intensity of PA6/PS/(SMA–CB) composites was not only stronger than that of PA6/PS/CB, but also their NTC effect was eliminated. The elimination of NTC effect was arisen from the especial interface morphology: SMA as well as the CB particles grafted on SMA molecular chains both localize at interphase to form the conductive pathways. The stronger PTC intensity was attributed to the lower percolation threshold and especial conductive morphology.

Acknowledgments The authors gratefully acknowledge the financial support of this study by the National Natural Science Foundation of China (Contract Number: 51003024) and the Foundation for University Young Key Teacher of He' Nan Province.

References

1. Strumpler R, Glatz-Reichenbach J (1999) Conducting polymer composites. J Electroceram 3(4):329–346
2. Huang JC (2002) Carbon black filled conducting polymers and polymer blends. Adv Polym Technol 21(4):299–313
3. Sumita M, Sakata K, Hayakawa Y, Asai S, Miyasaka K, Tanemura M (1992) Double percolation effect on the electrical conductivity of conductive particles filled polymer blends. Colloid Polym Sci 270(2):134–139
4. Zhang MQ, Gang YH, Zeng M, Zhang HB, Hou YH (1998) Two-step percolation in polymer blends filled with carbon black. Macromolecules 31(19):6724–6726
5. Yui H, Wu GZ, Sano H, Sumita M, Kino K (2006) Morphology and electrical conductivity of injection-molded polypropylene/carbon black composites with addition of high-density polyethylene. Polymer 47(10):3599–3608
6. Xu ZB, Zhao C, Gu AJ, Fang ZP (2007) Effect of morphology on the electric conductivity of binary polymer blends filled with carbon black. J Appl Polym Sci 106(3):2008–2017
7. Gubbels F, Jerome R, Teyssie PH, Vanlathem E, Deltour R, Calderone A (1994) Selective localization of carbon black in immiscible polymer blends: a useful tool to design electrical conductive composites. Macromolecules 27(7):1972–1974
8. Xu SX, Wen M, Li J, Guo SY, Wang M, Du Q (2008) Structure and properties of electrically conducting composites consisting of alternating layers of pure polypropylene and polypropylene with a carbon black filler. Polymer 49(22):4861–4870
9. Sumita M, Sakata K, Asai S, Miyasaka K, Nakagawa H (1991) Dispersion of fillers and the electrical conductivity of polymer blends filled with carbon black. Polym Bull 25(2):265–271
10. Gubbels F, Jerome R, Vanlathem E, Deltour R, Blacher S, Brouers F (1998) Kinetic and thermodynamic control of the selective localization of carbon black at the interface of immiscible polymer blends. Chem Mater 10(5):1227–1235

11. Dai K, Xu XB, Li ZM (2007) Electrically conductive carbon black (CB) filled in situ microfibrillar poly (ethylene terephthalate) (PET)/polyethylene (PE) composite with a selective CB distribution. Polymer 48(3):849–859
12. Feng J, Chan CM, Li JX (2003) A method to control the dispersion of carbon black in an immiscible polymer blend. Polym Eng Sci 43(5):1058–1063
13. Al-Saleh MH, Sundararaj U (2008) Nanostructured carbon black filled polypropylene/polystyrene blends containing styrene–butadiene–styrene copolymer: influence of morphology on electrical resistivity. Eur Polym J 44(7):1931–1939
14. Feng JY, Chan CM (2000) Positive and negative temperature coefficient effects of an alternating copolymer of tetrafluoroethylene–ethylene containing carbon black-filled HDPE particles. Polymer 41:7279–7282
15. Ahmad A, Mohd DHJ, Abdullah I (2004) Electron beam irradiation of carbon black filled linear low-density polyethylene. J Mater Sci 39(4):1459–1461
16. Xie HF, Deng PY, Dong LS, Sun JZ (2002) LDPE/carbon black conductive composites: influence of radiation crosslinking on PTC and NTC properties. J Appl Polym Sci 85(13):2742–2749
17. Lee GJ, Han MG, Chung SC, Suh KD, Im SS (2002) Effect of crosslinking on the positive temperature coefficient stability of carbon black-filled HDPE/ethylene–ethylacrylate copolymer blend system. Polym Eng Sci 42(8):1740–1747
18. Bin Y, Xu C, Zhu D, Matsuo M (2002) Electrical properties of polyethylene and carbon black particle blends prepared by gelation/crystallization from solution. Carbon 40(2):195–199
19. Xi Y, Ishikawa H, Bin YZ, Matsuo M (2004) Positive temperature coefficient effect of LMWPE–UHMWPE blends filled with short carbon fibers. Carbon 42:1699–1706
20. Feng JY, Chan CM (2000) Double positive temperature coefficient effects of carbon black-filled polymer blends containing two semicrystalline polymers. Polymer 41(12):4559–4565
21. Wang GJ, Qu ZH, Guo JL, Li Y, Liu L (2006) Study of multiple-wall carbon nanotubes functionalized by the poly(styrene-*co*-maleic anhydride). Acta Chim Sin 64(24):2505–2509
22. Meyer J (1973) Glass transition temperature as a guide to selection of polymers suitable for PTC materials. Polym Eng Sci 13:462–486
23. Ohe K, Naito Y (1971) A new resistor having an anomalously large positive temperature coefficient. Jpn J Appl Phys 10:99–108
24. Voet A (1981) Temperature effect of electrical resistivity of carbon black filled polymers. Rubber Chem Technol 54:42–50